

$L_{2,3}-M_{4,5}M_{4,5}$ Auger-electron spectra of the metallic elements $_{47}\text{Ag}$ to $_{51}\text{Sb}$: An analysis of the main and satellite structures

J.-M. Mariot

*Laboratoire de Chimie Physique, Université Pierre et Marie Curie, 11 rue Pierre et Marie Curie,
F-75231 Paris Cédex 05, France*

M. Ohno*

Institute of Theoretical Physics, Chalmers University of Technology, S-412 96 Göteborg, Sweden

(Received 10 February 1986)

The $L_{2,3}-M_{4,5}M_{4,5}$ Auger-electron spectra of the metallic elements $_{47}\text{Ag}$ to $_{51}\text{Sb}$ have been measured. The spectra are analyzed within the framework of Hartree-Fock differential self-consistent-field (ΔSCF) calculations in which correlation and relativistic energy shifts have been included, using $j-j$ coupling for the initial state and intermediate coupling for the final state. It is found that structure on the low-energy side of the $L_3-M_{4,5}M_{4,5}$ spectrum, previously interpreted as due to the $L_3M_{4,5}-M_{4,5}M_{4,5}M_{4,5}$ multiple-hole excitations following the $L_1-L_3M_{4,5}$ Coster-Kronig decay process, is also present in the $L_2-M_{4,5}M_{4,5}$ spectrum. Electron energy-loss spectroscopy data show that the structure in fact corresponds to plasmon satellites. The $L_3M_{4,5}-M_{4,5}M_{4,5}M_{4,5}$ satellites are revealed in $_{47}\text{Ag}$ and $_{48}\text{Cd}$ by an anomalous value of the intensity ratio of the $L_3-M_{4,5}M_{4,5}$ and $L_2-M_{4,5}M_{4,5}$ groups. The $L_{2,3}$ level widths of the elements $_{47}\text{Ag}$ to $_{51}\text{Sb}$ are determined from a simulation of the experimental spectra using our theoretical results.

I. INTRODUCTION

Satellites appearing in x-ray emission spectroscopy (XES), x-ray photoelectron spectroscopy (XPS), and Auger-electron spectroscopy (AES) measurements provide useful information about the dynamics of multiple-hole excitations associated with the initial single-hole excitation. The theoretical analysis of the satellite structure is generally very complicated because of the presence of one or more extra holes. However, a qualitative analysis may provide sufficient knowledge about the presence or absence of particular decay channels for the initial single-hole state. This may be obtained from the observation of changes in satellite intensities as the excitation energy is driven above or below the initial single-hole ionization energy threshold, by changing the environment (e.g., from free atoms to metals), or by examining changes as a function of the atomic number. An increase (or a decrease) in the XPS spectrum linewidth provides direct evidence for the opening (or closing) of decay channels. If such direct evidence is not available, the XES and AES satellite measurements can also contribute sufficient information (see Refs. 1–4 for experimental and theoretical work in this respect). A good example is the extensive experimental and theoretical work carried out on the $L_{2,3}$ XPS, the $L_{2,3}-M_{4,5}M_{4,5}$ AES and the $L_{2,3}$ XES spectra of the elements $_{29}\text{Cu}$ to $_{32}\text{Ge}$.^{3,5–14} These spectra show that $L_2-L_3M_{4,5}$ Coster-Kronig (CK) processes are forbidden in atomic Cu and Zn, but are allowed in metallic Cu and Zn due to the atom-solid CK energy shift. This is directly confirmed by a decrease of the L_2 XPS linewidth when going from the metal to the free atom.^{5,6,8} Furthermore, this is indirectly confirmed by a decrease in the free atom of the satellite intensities in the $L_3-M_{4,5}M_{4,5}$ AES spec-

tra^{2,7,9} and in the $L\alpha_{1,2}$ ($L_3-M_{5,4}$) XES spectra^{10,11} due to the closing of the $L_2-L_3M_{4,5}-M_{4,5}M_{4,5}$ cascade. Theoretically, this is confirmed for the atomic case by ΔSCF calculations of the atomic $L_2-L_3M_{4,5}$ CK energy^{12,13} and for the solid-state case both by a semiempirical calculation of the solid-state $L_2-L_3M_{4,5}$ CK energy¹⁴ and by recent atom-solid CK energy-shift calculations.³

The absence or presence of particular CK decay channels can also be studied systematically by increasing the atomic number. Such an approach has shown that the $L_1-L_3M_{4,5}$ CK decay channels are forbidden when we reach atomic and metallic $_{50}\text{Sn}$. The L_1 XPS spectra of the elements neighboring Sn, which would provide direct evidence for the closing of the $L_1-L_3M_{4,5}$ CK decay channels, are not available so far. Nevertheless, the $L\beta_{3,4}$ ($L_1-M_{3,2}$) XES spectra do indicate the closing of the $L_1-L_3M_{4,5}$ CK decay channels at Sn since the L_1 linewidths determined from the $L\beta_{3,4}$ XES spectra show a drop at Sn.⁴ A sharp drop has also been observed at Sn for the ratio of the $L\alpha_1$ satellite intensity to the total $L\alpha_1$ (L_3-M_5) x-ray emission intensity measured with 2.5-MeV proton bombardment.^{15,16} An intensity increase was observed in the satellite region of the Ag $L\alpha_1$ XES spectrum as the energy of the primary excitation was increased above the L_1 ionization energy.^{17,18} This $L\alpha_1$ XES satellite was interpreted as due to the $L_1-L_3M_{4,5}-M_{4,5}M_{4,5}$ cascade which closes at Sn.^{19,20} The $L_3-M_{4,5}M_{4,5}$ AES spectra of the elements in the vicinity of Sn are also expected to show a variation in satellite intensity due to the closing or opening of the $L_1-L_3M_{4,5}-M_{4,5}M_{4,5}M_{4,5}$ cascade. The $L_3-M_{4,5}M_{4,5}$ AES spectrum of metallic Ag has been measured with this point in mind.²¹ A structure on the low-energy side of the main peak was observed and interpreted as a satellite resulting from the

$L_1\text{-}L_3M_{4,5}\text{-}M_{4,5}M_{4,5}M_{4,5}$ cascade.

In this paper, we report on the first systematic study of the $L_{2,3}\text{-}M_{4,5}M_{4,5}$ AES spectra in metallic $_{47}\text{Ag}$ to $_{51}\text{Sb}$ in order to elucidate the origin of this structure. After a brief description of the experimental conditions (Sec. II), an analysis of the Auger spectra is presented (Sec. III). Energy (Sec. IIIA) and intensity (Sec. IIIB) calculations are discussed. Placing the emphasis on satellite structures, we compare the results of our theoretical model with experiment (Sec. IIIC). The energies of the $L_3M_{4,5}\text{-}M_{4,5}M_{4,5}M_{4,5}$ Auger satellite transitions are calculated and the existence of such satellites is discussed in Sec. IIID. Finally, the $L_{2,3}$ level widths we have determined from our experiments are given and compared with other available data (Sec. III E). Conclusions are drawn in Sec. IV.

II. EXPERIMENTAL

The Auger spectra induced by the 14-kV bremsstrahlung emitted by an Al anode were analyzed using the electron optics (electrostatic retarding lens and hemispherical analyzer) of an AEI ES 200 B spectrometer operated at a resolving power of ~ 1500 . Spectroscopically pure foils mechanically scraped under vacuum were used as samples. The spectra reported here were obtained from samples for which the oxygen and carbon contamination was estimated to be less than a few percent of a monolayer. The energy scale was calibrated in the following way: a gold sample suitably biased using a 0.005% stabilized high-voltage supply was used to produce photoelectrons of known energies in the range of interest; the exact value of the bias was measured by feeding the high voltage to a precision digital voltmeter through a calibrated voltage divider; a value of 83.8 eV was taken for the binding energy of the Au $4f_{7/2}$ level used for the calibration.

The energy losses suffered by the Auger electrons on their way out to the vacuum strongly influence the shape of high-energy Auger spectra. In order to be able to make a detailed comparison between the experimental Auger spectra and those predicted by our calculations, a knowledge of the electron energy-loss data for each sample was needed. This was accomplished by bombarding the sample with monochromatic electrons having an energy close to that of the Auger electrons and by studying the energy spectra of the reflected electrons. These were found to be in good agreement with previously reported spectra.²²⁻²⁴

III. RESULTS AND DISCUSSION

A. $L_{2,3}\text{-}M_{4,5}M_{4,5}$ Auger energies in the metals

The holes involved in the $L_{2,3}\text{-}M_{4,5}M_{4,5}$ Auger processes are localized on a core atomic site. Thus the atomic approach is relevant for an analysis of the spectra. First of all, we calculate the atomic Auger energy. One of the simple ways to calculate approximately the atomic Auger energy is the Hartree-Fock (HF) ΔSCF method. One calculates the total energy of the initial single-hole state and that of the final double-hole state within the HF scheme. It is known that the HF ΔSCF method often

gives good agreement (to within ~ 1 eV) with the experimental atomic ionization energy. This does not necessarily mean that the HF ΔSCF provides the accurate atomic ionization energy. One should take into consideration the following points at least when one performs the ΔSCF calculations and compares them with experiment.

(1) The calculation of the total energy often involves numerical inaccuracy which tends to cancel out when we obtain the ΔSCF results.

(2) The HF scheme completely neglects the correlation. When the initial- and final-state correlations are almost the same, the discrepancy between the experiment and the HF ΔSCF result is quite small and is interpreted, when $|E(\text{expt})| > |E(\Delta\text{SCF})|$, as the ground-state correlation, which is of the order of 1 eV. The HF ΔSCF scheme describes only the monopole relaxation [i.e., radial redistribution of the surrounding electron clouds to the sudden creation of a hole (or holes)].²⁵ When the angular (non-radial) distortion of the system is involved, e.g., dipole relaxation, the ΔSCF energy exceeds appreciably the experimental energy ($\sim 2\text{--}3$ eV, sometimes as much as 10 eV). This kind of relaxation has to be treated in a perturbative way. The perturbative treatment by a HF scheme generally very much improves the results, although it often tends to be nonsystematic in a strict sense when one tries to take into account the higher-order terms.

Here, as the dipole relaxation of both initial $L_{2,3}$ and final $M_{4,5}M_{4,5}$ hole states is negligible (this we deduce from the agreement between the relativistic ΔSCF results and the atomic experimental data for a single $2p$ or $3d$ hole level) and since we are not aiming at calculating the metallic $L_{2,3}\text{-}M_{4,5}M_{4,5}$ Auger energies with high accuracy, we limited ourselves to the HF ΔSCF calculations. We correct the ΔSCF Auger energy by adding the relativistic energy shift and the ground-state correlation energy shift. For the $M_{4,5}M_{4,5}$ double-hole energy, the relativistic effect can be obtained as twice the difference between the Dirac-Hartree-Fock (DHF) and HF eigenvalues for a single $M_{4,5}$ hole, because the energy corrections due to Breit interaction, vacuum polarization, self-energy, and quantum-electrodynamic effects are negligible. In the case of the $L_{2,3}$ hole state, as the Breit interaction becomes large (~ 9.5 and ~ 6.9 eV for the L_2 and L_3 hole states of cadmium²⁶), we use the Dirac-Hartree-Fock-Slater (DHFS) ΔSCF energies calculated by Huang *et al.*²⁶ The ground-state correlation energy shift can be obtained by comparing the DHFS energies²⁶ with the atomic experimental data. For the levels where the atomic data are not available, we estimate the atomic energies from the solid-state level using the atom-solid energy shift Δ^{AS} calculated by Johansson and Mårtensson,²⁷ which is accurate to within 0.5 eV. The atom-solid energy shift Δ^{AS} can be expressed²⁸ as the sum of a chemical shift, of an energy shift due to configuration change, of an extra-atomic relaxation shift Δ^{ext} , and of the work function. For core levels, we may consider that Δ^{AS} and Δ^{ext} are approximately level independent. Then it can be shown^{3,28} that the metallic Auger energy E^{S} (referenced with respect to the Fermi level) can be obtained from the atomic Auger energy E^{A} by

$$E^{\text{S}} = E^{\text{A}} + \Delta^{\text{AS}} + 2\Delta^{\text{ext}}. \quad (1)$$

In the equivalent core approximation, the extra-atomic relaxation shift may be obtained by²⁹

$$\Delta^{\text{ext}} \simeq \frac{1}{2} [F^0(i, j)]_{Z+1}, \quad (2)$$

where i denotes the hole and j the screening electron. Here, for the sake of accuracy and assuming that Δ^{ext} is not affected by the presence of an extra hole, we have used the Δ^{AS} obtained in a semiempirical way by Aksela *et al.*³⁰ for the $3d_{5/2}$ level (typically 7.6 eV for Ag) and the Δ^{ext} obtained from Eq. (1) for the $M_{4,5}-N_{4,5}N_{4,5}$ (1G_4) Auger energy²⁸ (typically 4.5 eV for Ag).

For the elements of interest here (except Cd) the atomic approach we use to calculate the solid-state Auger energies should in principle take into account the coupling between the initial $2p_{1/2}$ or $2p_{3/2}$ hole state and the final $3d^{-2}$ double-hole state with the outermost shell (open shell) electrons. We performed the DHF Δ SCF calculations for the $2p_{1/2,3/2}$ and $3d^{-2}$ hole levels by using Grant's code,³¹ with intermediate coupling and without configuration interaction. In most cases (particularly for the $3d$ holes), the coupling generates many multiplets which makes the analysis of the spectra difficult. However, our results indicate that the inclusion of the coupling does not change drastically the Auger energies. Moreover, it should be noted that the coupling between the initial hole and the final holes with the valence electrons is expected to be very weak since the XPS spectra give no evidence of multiplet splitting. Thus our present scheme without coupling is sufficient for the analysis of the present Auger spectra.

B. $L_{2,3}-M_{4,5}M_{4,5}$ Auger intensities

As the $L_{2,3}-M_{4,5}M_{4,5}$ Auger processes are localized on the atomic site, an atomic intensity calculation should be suitable. We calculate the intensities by using the radial Auger matrix elements obtained by McGuire³² and by assuming $j-j$ coupling in the initial state and intermediate coupling in the final state.

The calculations by McGuire often give quite good agreement for the Auger decay rates; however, they overestimate the CK rates by a factor of $\sim 2-3$. We leave further detailed discussion of the origin of this discrepancy to the work reported elsewhere by one of us.³³⁻³⁶ Here we will point out that, in general, the Auger decay matrix elements calculated by the HF scheme are changing slowly with the decay energy in contrast to the CK decay matrix elements which tend to change rapidly with the CK decay energy because the CK energy often falls in the near-threshold region. Furthermore, the Auger matrix elements are often rather insensitive to the choice of potential, basis set, etc., in contrast to the CK decay matrix elements. Thus the use of McGuire's results for an analysis of the Auger transitions involved here is relevant.

C. Comparison between theory and experiment

The $L_3-M_{4,5}M_{4,5}$ and $L_2-M_{4,5}M_{4,5}$ spectra of metallic $_{47}\text{Ag}$ to $_{51}\text{Sb}$ are shown in Figs. 1 and 2, respectively. The spectra of each group have been aligned on the most intense peak (1G_4). They have also been normalized to the

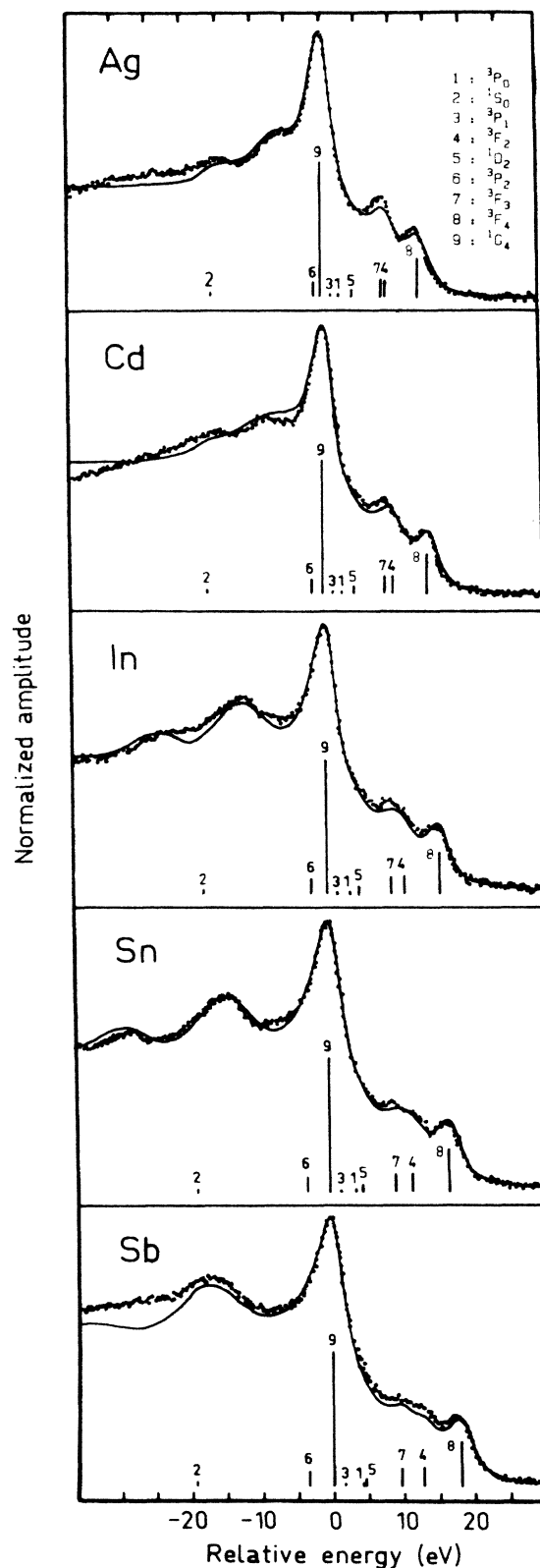


FIG. 1. $L_3-M_{4,5}M_{4,5}$ Auger spectra of the metallic elements $_{47}\text{Ag}$ to $_{51}\text{Sb}$. The experimental spectrum (dotted curve) is compared with the simulated spectrum (solid line) that can be obtained from the results of our calculations (bars) using electron energy-loss data.

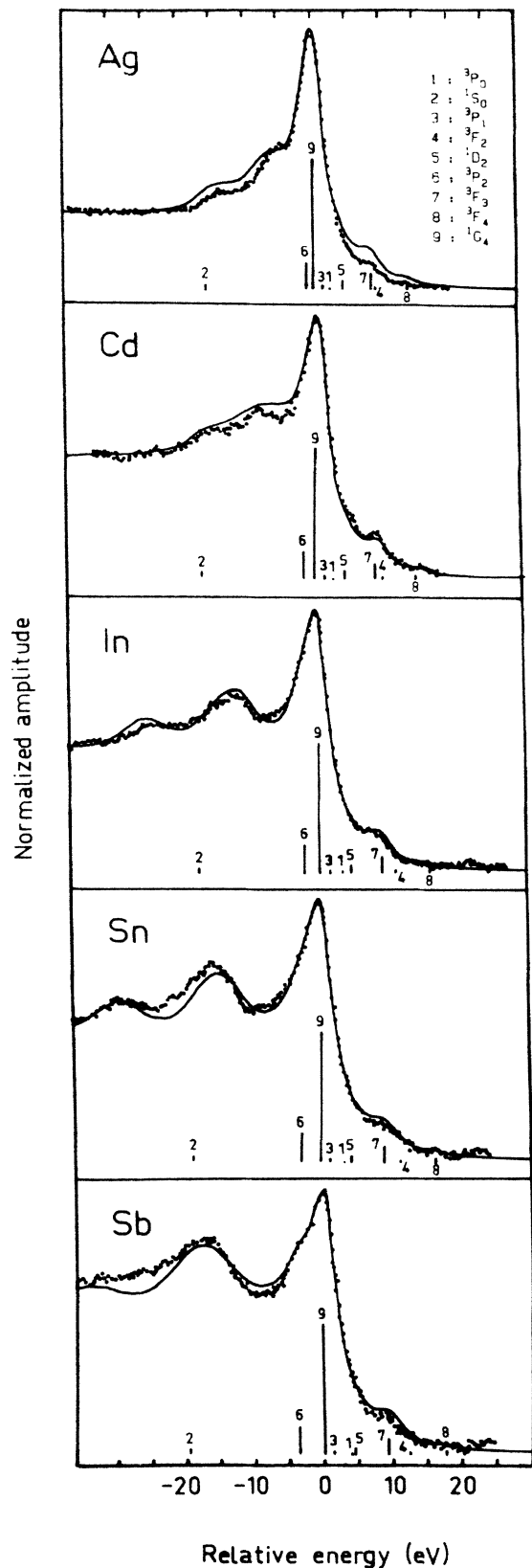


FIG. 2. $L_{2,3}-M_{4,5}M_{4,5}$ Auger spectra of the metallic elements $_{47}\text{Ag}$ to $_{51}\text{Sb}$. See caption of Fig. 1 for details.

maximum amplitude of this peak. The energies relative to the 1G_4 peak and the relative intensities given by our calculations are also given in the figures. It is seen that the evolution of the splittings observed in the spectra is well accounted for by our calculations. Theory also explains well the differences in intensity between the L_3 and L_2 groups, namely the almost complete disappearance of the 3F_4 and 3F_2 transitions as well as the greater intensity of the 3P_2 transition when going from the L_3 to the L_2 groups. The absolute Auger energies we have calculated for the 1G_4 peak are about 3 eV smaller than the measured energies (see Table I).

We give also in Table I the DF Δ SCF solid-state Auger energies calculated for $_{48}\text{Cd}$ with intermediate coupling and without configuration interaction using a relativistic code.³¹ The results are in good agreement with experiment. This is mainly due to the proper treatment of the relativistic effects, i.e., Breit interaction, vacuum polarization, self-energy, and quantum-electrodynamic corrections. The larger discrepancy between the nonrelativistic Δ SCF results with relativistic corrections and experiment is possibly due to the relativistic corrections introduced in the present work and to differences in the Coulomb integrals. Note that the Coulomb integrals used in the relativistic approach are calculated for the final double-hole configuration in contrast to those used in the nonrelativistic approach, which are obtained for the neutral ground state. In principle, one should use the Coulomb integrals of the neutral ground state in order to treat the relaxation in the presence of the final double holes in a perturbing way. But as monopole screening shifts the average final double-hole energies but not much the term splittings, our choice of the 1G_4 transition for the comparison is a matter of convenience.

The importance of relativity and correlation effects in the L - MM Auger spectra has been recently discussed by Chen,³⁷ who performed Dirac-Hartree-Slater calculations in intermediate coupling with configuration interaction for selected elements with atomic numbers $18 \leq Z \leq 92$. When corrections for correlation effects are taken into account, these calculations are in excellent agreement with the experimental data available. Unfortunately, our results cannot be compared with those of Chen because the Auger spectra reported here were not studied by him.

From Table I it is also seen that the semiempirical solid-state Auger energies obtained by Larkins³⁸ are 5–6 eV lower than the experimental energies. These differences seem to be somewhat too large even when we take into account the uncertainty of experimental binding energies which besides tends to cancel out in the evaluation of the Auger energy. We consider that the main cause of discrepancies is due to the "solid-state correction term" evaluated by the atomic HF screening model used by Larkins.^{38,39} This solid-state correction term corresponds to the term $2\Delta^{\text{ext}}$ of Eq. (1), as well as to the last two terms of Eq. (41) in Ref. 28. (Note that the extra-atomic relaxation defined here and in Ref. 28 is different from the "incorrect definition" which is usually taken as the total atom-solid energy shift minus work function.) If we take the semiempirical extra-atomic relaxation shift obtained in Ref. 28, we find that the discrepancy between the

TABLE I. Measured and calculated $L_{2,3}\text{-}M_{4,5}M_{4,5}$ (1G_4) Auger energies (eV) of the metallic elements $_{47}\text{Ag}$ to $_{51}\text{Sb}$. The experimental uncertainty is estimated to be 0.7 eV.

Element	Initial hole-state	Expt.	Auger energy		
			This work	Ref. 38	Ref. 38 ^a
$_{47}\text{Ag}$	L_2	2750.3	2749.5	2746.3	2746.6
	L_3	2578.0	2576.7	2573.7	2574.0
$_{48}\text{Cd}$	L_2	2877.1	2872.8 2876.2 ^b	2870.3	2873.7
	L_3	2687.1	2683.1 2686.4 ^b	2680.8	2684.2
$_{49}\text{In}$	L_2	3007.1	3004.4	3000.8	3004.1
	L_3	2799.7	2796.5	2792.9	2796.2
$_{50}\text{Sn}$	L_2	3140.1	3137.2	3133.8	3136.9
	L_3	2912.8	2909.7	2906.6	2909.7
$_{51}\text{Sb}$	L_2	3276.0	3272.0	3271.1	3273.0
	L_3	3027.8	3023.7	3022.9	3024.8

^aWith extra-atomic relaxation of Ref. 28.

^bFrom DHF ΔSCF calculations (see text).

semiempirical and experimental Auger energies reduces to 1–4 eV (see Table I). The remaining discrepancy could be due to the uncertainty of the experimental data used in the semiempirical approach and to the assumption that the atom-solid Auger energy shift is level independent.

The energy losses suffered by the Auger electron on its path towards the vacuum have to be taken into account if a closer comparison between theory and experiment has to be made. This was done by associating the electron energy-loss structures corresponding to the element involved to each theoretical line and by summing up the contributions from the various transitions. Each loss spectrum was determined by fitting Gaussian-type structures superimposed on a suitable background to our electron energy-loss data and by broadening the fit so as to obtain an elastic peak width close to the 1G_4 linewidth. The spectra given by this simulation procedure are compared with experiment in Figs. 1 and 2. This comparison shows that loss processes explain well the structures observed on the low-energy side of the main (1G_4) line in both the L_3 and L_2 spectra. However, in some cases, the intensity ratio of the loss structures to the elastic peak has to be slightly decreased when going from the L_3 to the L_2 spectrum in order to get an intensity in the low-energy part of the simulated spectrum in agreement with experiment. This is an indication that extra structures are present in the low-energy part of the $L_3\text{-}M_{4,5}M_{4,5}$ spectrum (see Sec. III D).

D. $L_3M_{4,5}\text{-}M_{4,5}M_{4,5}M_{4,5}$ Auger satellites

In order to see approximately in which energy region the $L_3M_{4,5}\text{-}M_{4,5}M_{4,5}$ satellites fall, we calculated the solid-state $L_3M_{4,5}\text{-}M_{4,5}M_{4,5}$ satellite energies for the elements in which the $L_1\text{-}L_3M_{4,5}$ CK transition is allowed ($Z < 50$). The atomic satellite energy can be ob-

tained approximately by³

$$E^A(LM\text{-}MMM) \simeq E_{MMM}(\Delta\text{SCF}) - E_{LM}(\Delta\text{SCF}) + \Delta_M^C, \quad (3)$$

where $E(\Delta\text{SCF})$ are ΔSCF energies (negative) and Δ_M^C is the ground-state correlation energy shift of an M -shell hole (here we assume that the ground-state correlation energy is almost level independent and the ground-state correlation energy of multiple holes is a linear sum of that of the single holes). We calculate the nonrelativistic HF $L_3M_{4,5}\text{-}M_{4,5}M_{4,5}$ ΔSCF energies and make the relativistic energy shift corrections. The solid-state $L_3M_{4,5}\text{-}M_{4,5}M_{4,5}$ satellite energy is then deduced from the atomic one by³

$$E^S(LM\text{-}MMM) \simeq E^A(LM\text{-}MMM) + \Delta_{MMM} - \Delta_{LM} + \phi. \quad (4)$$

Here Δ_{LM} and Δ_{MMM} are the atom-solid energy shift (referenced to the vacuum level) of the two and three holes, and ϕ is the work function.⁴⁰ We approximate the atom-solid energy shift of two and three holes by³

$$\Delta_{MMM} - \Delta_{LM} \simeq (\Delta^{\text{AS}} - \phi) + 4\Delta^{\text{ext}}. \quad (5)$$

The calculated solid-state satellite energies are given in Table II.

The $L_{2,3}\text{-}M_{4,5}M_{4,5}$ AES spectra of the metallic elements Ag to Sb do not show marked structure corresponding to $L_3M_{4,5}\text{-}M_{4,5}M_{4,5}$ satellites. According to our calculations, the energy range of the satellite transitions is rather broad (~ 30 eV). So these transitions may contribute to the intensity only as a smooth background. In order to detect its presence we have estimated the intensity ratio $I(L_3\text{-}M_{4,5}M_{4,5})/I(L_2\text{-}M_{4,5}M_{4,5})$ for each element. The values obtained, which are given in Table II, indicate that unresolved Auger satellite emissions are

TABLE II. The $L_{2,3}M_{4,5}M_{4,5}M_{4,5}M_{4,5}$ Auger satellites in the metallic elements $_{47}\text{Ag}$ to $_{51}\text{Sb}$: calculated energies (eV) for the elements in which the $L_1-L_3M_{4,5}$ CK process is allowed ($Z < 50$) and measured intensity ratios of the $L_3-M_{4,5}M_{4,5}$ and $L_2-M_{4,5}M_{4,5}$ groups (the estimated errors on these ratios are given in parentheses).

Element	Auger satellite	
	energy	$\frac{I(L_3-M_{4,5}M_{4,5})}{I(L_2-M_{4,5}M_{4,5})}$
$_{47}\text{Ag}$	2540.8–2572.5	2.24(0.20)
$_{48}\text{Cd}$	2647.2–2680.0	2.32(0.15)
$_{49}\text{In}$	2757.2–2791.8	2.01(0.20)
$_{50}\text{Sn}$		1.85(0.20)
$_{51}\text{Sb}$		2.07(0.15)

present in $_{47}\text{Ag}$ and $_{48}\text{Cd}$ since the intensity ratio is greater than the ratio of the statistical weight of the L_3 and L_2 levels for these elements. The accuracy ($\sim 10\%$) of the intensity ratio is not sufficient however to determine the exact cutoff atomic number for the $L_1-L_3M_{4,5}$ CK process.

Since the intensity variation in the satellite energy region is not very pronounced, the $L_1-L_3M_{4,5}M_{4,5}M_{4,5}M_{4,5}$ cascade is weak in the elements $_{47}\text{Ag}$ to $_{51}\text{Sb}$ in contrast to the case of the $L_2-L_3M_{4,5}$ -

$M_{4,5}M_{4,5}M_{4,5}$ cascade for the elements $_{29}\text{Cu}$ to $_{32}\text{Ge}$. But it should be noted that the $3d$ holes in the elements around Sn are much more strongly localized on the atomic site than in the case of the elements around $_{30}\text{Zn}$. The presence of localized $3d$ holes can pull the continuum wave function of the Auger electron inwards. As the Auger energy of interest here is high, this results in the reduction of radial integral parts of the $L_3M_{4,5}M_{4,5}M_{4,5}M_{4,5}$ decay rates. In the case of $L_1-L_3M_{4,5}M_{4,5}M_{4,5}$ multiple-hole excitations associated with the $L_3-M_{4,5}$ x-ray emission processes, the dipole matrix elements are determined by the occupied orbitals ($2p_{3/2}$, $3d$ levels) which may not be influenced very much by the presence of a localized $3d$ extra hole. This could explain why the satellites are more clearly visible in the XES than in the AES spectra. However, further detailed theoretical and experimental analysis is necessary to provide a more concrete explanation.

E. $L_{2,3}$ level widths

The simulation procedure used to compare theory with experiment also allows the widths of the $L_{2,3}$ levels to be determined. For this determination it was assumed that the true width G of an Auger line located at the energy E is related to the observed width G_{obs} by

$$G = [G_{\text{obs}}^2 - (E/R)^2]^{1/2}, \quad (6)$$

TABLE III. Experimental and theoretical $L_{2,3}$ level widths (eV) of the metallic elements $_{47}\text{Ag}$ to $_{51}\text{Sb}$.

Element	Level	Experiment		Ref. 49	Theory	
		This work ^a	Others		Ref. 50	Ref. 51
$_{47}\text{Ag}$	L_2	2.22 ± 0.21	$2.42,$ ^b $2.06,$ ^c $2.20,$ ^d 2.32 ± 0.25 ^e	2.57	2.57	2.32
	L_3	2.22 ± 0.21	$2.32,$ ^b $1.77,$ ^c $2.0,$ ^d $2.2,$ ^f $1.9 \pm 0.3,$ ^g 2.14 ± 0.25 ^e	2.12	2.40	2.15
$_{48}\text{Cd}$	L_2	2.13 ± 0.21	$2.15,$ ^c 2.39 ± 0.25 ^e		2.62	
	L_3	2.13 ± 0.21	$2.10,$ ^h 2.36 ± 0.25 ^e		2.50	
$_{49}\text{In}$	L_2	2.56 ± 0.21	$2.25,$ ^c $2.2 \pm 0.4,$ ⁱ 2.65 ^e		2.72	
	L_3	2.56 ± 0.21	$1.95,$ ^c $2.1 \pm 0.4,$ ⁱ 2.50 ^e		2.65	
$_{50}\text{Sn}$	L_2	2.61 ± 0.21	$3.17,$ ^c $2.1 \pm 0.4,$ ⁱ 2.61 ^e		2.84	2.64
	L_3	2.61 ± 0.21	$2.05,$ ^c $2.65,$ ^j 2.47 ^e		2.75	2.43
$_{51}\text{Sb}$	L_2	2.67 ± 0.21	$2.4 \pm 0.4,$ ¹ 2.64 ^e		3.00	
	L_3	2.67 ± 0.21	2.2 ± 0.4 ⁱ			

^aThe error on the width of the 1G_4 Auger line is estimated to be 0.20 eV, the error on the $M_{4,5}$ level width being only 0.05 eV (see Ref. 41).

^bReference 42.

^cReference 43.

^dReference 44.

^eReference 4.

^fReference 45.

^gReference 18.

^hReference 46.

ⁱReference 47.

^jReference 48.

where R is the resolving power of the spectrometer and G is the sum of the widths of the levels involved in the transition. The values so obtained using the $M_{4,5}$ level widths measured by XPS by Mårtensson and Nyholm⁴¹ are given in Table III. They are also compared in this table with other experimental values^{4,42-48} and with theoretical results.⁴⁹⁻⁵¹ For a detailed discussion of the origin of the various experimental data we refer to the recent work of Putila-Mäntylä *et al.*⁴ The theoretical results obtained by McGuire⁴⁹ and Chen *et al.*,⁵¹ using, respectively, the basis set generated by Herman-Skillman and Dirac-Hartree-Slater V^{N-1} potentials, are in good agreement with the experimental $L_{2,3}$ widths. This seems (see, e.g., Refs. 35-37) to be due to the fact that the $L_{2,3}$ holes decay mostly via Auger processes since, for the same elements, such a choice of basis sets fails to predict the L_1 widths which are almost entirely determined by CK processes.

IV. CONCLUSION

We have measured for the first time the $L_{2,3}-M_{4,5}M_{4,5}$ AES spectra of the metallic elements $_{47}\text{Ag}$ to $_{51}\text{Sb}$. The energies of the transitions are well accounted for by ΔSCF calculations with inclusion of correlation and relativistic

energy shifts. The structures on the low-energy side of the $L_3-M_{4,5}M_{4,5}$ AES spectra previously interpreted as the $L_3M_{4,5}-M_{4,5}M_{4,5}M_{4,5}$ satellites are also observed in the $L_2-M_{4,5}M_{4,5}$ spectra and correspond to plasmon satellites, as shown from a simulation based on intensity calculations performed using $j-j$ coupling in the initial one-hole state and intermediate coupling in the final two-hole state. The $L_3-M_{4,5}M_{4,5}$ AES spectra of $_{47}\text{Ag}$ and $_{48}\text{Cd}$ show an indication of the $L_3M_{4,5}-M_{4,5}M_{4,5}M_{4,5}$ multiple-hole excitations accompanying the $L_1-L_3M_{4,5}$ CK decay process. But these are less marked than those accompanying the $L_2-L_3M_{4,5}$ CK processes which are observed in the $L_3-M_{4,5}M_{4,5}$ AES spectra of the elements in the neighborhood of $_{30}\text{Zn}$. The widths of the $L_{2,3}$ levels have been deduced from our spectra and compared to other experimental and theoretical determinations.

ACKNOWLEDGMENTS

One of us (M.O.) is grateful to the Swedish Natural Science Research Council and to the Deutsche Forschungsgemeinschaft for financial support. The Laboratoire de Chimie Physique is "Unité No. 176 associé au Centre National de la Recherche Scientifique."

*Present address: Physikalisches Institut, Universität Bonn, Nussallee 12, D-5300 Bonn 1, Federal Republic of Germany.

¹R. D. Deslattes, R. E. La Villa, and A. Henins, *Nucl. Instrum. Methods* **152**, 179 (1978).

²P. Weightman, *Rep. Prog. Phys.* **45**, 753 (1982).

³M. Ohno, *J. Phys. C* **17**, 1437 (1984).

⁴P. Putila-Mäntylä, M. Ohno, and G. Graeffe, *J. Phys. B* **17**, 1735 (1984).

⁵L. I. Yin, I. Adler, M. H. Chen, and B. Crasemann, *Phys. Rev. A* **7**, 897 (1973).

⁶E. Antonides, E. C. Janse, and G. A. Sawatzky, *Phys. Rev. B* **15**, 4596 (1977).

⁷E. D. Roberts, P. Weightman, and C. E. Johnson, *J. Phys. C* **8**, L301 (1975).

⁸M. S. Banna, D. C. Frost, C. A. McDowell, and B. Wallbank, *J. Chem. Phys.* **68**, 596 (1978).

⁹S. Aksela, J. Väyrynen, and H. Aksela, *Phys. Rev. Lett.* **33**, 999 (1974).

¹⁰C. F. Hague, J.-M. Mariot, and H. Ostrowiecki, *Phys. Lett.* **67A**, 121 (1978).

¹¹C. F. Hague, J.-M. Mariot, and H. Ostrowiecki, *Jpn. J. Appl. Phys.* **17**, 105 (1978).

¹²M. H. Chen, B. Crasemann, K.-N. Huang, M. Aoyagi, and H. Mark, *At. Data Nucl. Data Tables* **19**, 97 (1977).

¹³H. Guennou, A. Sureau, G. Dufour, C. F. Hague, and J.-M. Mariot, in *Inner-Shell and X-Ray Physics of Atoms and Solids*, edited by D. J. Fabian, H. Kleinpoppen, and L. M. Watson (Plenum, New York, 1981), p. 797.

¹⁴F. P. Larkins, *J. Phys. C* **11**, 1965 (1978).

¹⁵B. L. Doyle and S. M. Shafroth, in *Abstracts of Contributed Papers of the Second International Conference on Inner-Shell Ionization Phenomena* (Universität Freiburg Press, Freiburg, 1976), p. 211.

¹⁶B. L. Doyle and S. M. Shafroth, *Phys. Rev. A* **19**, 1433 (1979).

¹⁷V. O. Kostroun, J.-P. Briand, A. Chetoui, P. Chevallier, and A. Touati (unpublished).

¹⁸C. F. Hague, J.-M. Mariot, and G. Dufour, *Phys. Lett.* **78A**, 328 (1980).

¹⁹M. H. Chen, B. Crasemann, M. Aoyagi, and H. Mark, *Phys. Rev. A* **15**, 2312 (1977).

²⁰J. Tulkki and O. Keski-Rahkonen, *Phys. Rev. A* **24**, 849 (1981).

²¹J.-M. Mariot, C. F. Hague, and G. Dufour, in *Inner-Shell and X-Ray Physics of Atoms and Solids*, edited by D. J. Fabian, H. Kleinpoppen, and L. M. Watson (Plenum, New York, 1981), p. 513.

²²C. J. Powell, *Proc. Phys. Soc. (London)* **76**, 593 (1960).

²³J. L. Robins, *Proc. Phys. Soc. (London)* **78**, 1177 (1961).

²⁴J. L. Robins, *Proc. Phys. Soc. (London)* **79**, 119 (1962).

²⁵G. Wendin and M. Ohno, *Phys. Scr.* **14**, 148 (1976).

²⁶K.-N. Huang, M. Aoyagi, M. H. Chen, B. Crasemann, and H. Mark, *At. Data Nucl. Data Tables* **18**, 243 (1976).

²⁷B. Johansson and N. Mårtensson, *Phys. Rev. B* **21**, 4427 (1980).

²⁸M. Ohno and G. Wendin, *J. Phys. C* **15**, 1787 (1982).

²⁹D. A. Shirley, *Phys. Rev. A* **7**, 1520 (1973).

³⁰S. Aksela, R. Kumpula, H. Aksela, and J. Väyrynen, *Phys. Scr.* **25**, 45 (1982).

³¹I. P. Grant, B. J. McKenzie, P. H. Norrington, D. F. Mayers, and N. C. Pyper, *Comput. Phys. Commun.* **21**, 207 (1980).

³²E. J. McGuire, Sandia Laboratories Research Report No. SC-RR-710075, 1971 (unpublished).

³³M. Ohno and G. Wendin, *Phys. Rev. A* **31**, 2318 (1985), and the references cited therein.

³⁴M. Ohno, *J. Phys. B* **17**, 195 (1984).

³⁵M. Ohno, *Phys. Rev. B* **29**, 3127 (1984).

³⁶M. Ohno and G. Wendin, *J. Phys. B* **12**, 1305 (1979).

³⁷M. H. Chen, *Phys. Rev. A* **31**, 177 (1985).

³⁸F. P. Larkins, *At. Data Nucl. Data Tables* **20**, 211 (1977).

³⁹F. P. Larkins, *J. Phys. C* **10**, 2461 (1977).

⁴⁰Values of work functions were taken from, *CRC Handbook of Chemistry and Physics*, 65th ed., edited by R. C. Weast (CRC,

Boca Raton, Florida, 1984), p. E-76.

⁴¹N. Mårtensson and R. Nyholm, Phys. Rev. B **24**, 7121 (1980).

⁴²M. A. Blokhin and V. P. Sachenko, Bull. Acad. Sci. USSR **21**, 1333 (1957).

⁴³B. G. Gokhale, Ann. Phys. (Paris) **7**, 852 (1952).

⁴⁴L. G. Parratt, Phys. Rev. **54**, 99 (1938).

⁴⁵L. G. Parratt, Rev. Mod. Phys. **31**, 616 (1959).

⁴⁶J. S. Geiger, R. L. Graham, and J. S. Merritt, Nucl. Phys. **48**,

97 (1963).

⁴⁷E. Noreland, Ark. Fys. **26**, 341 (1964).

⁴⁸A. Meisel and W. Nefedow, Ann. Phys. (Leipzig) **9**, 48 (1961).

⁴⁹E. J. McGuire, Phys. Rev. A **3**, 1801 (1971).

⁵⁰M. O. Krause and J. H. Oliver, J. Phys. Chem. Ref. Data **8**, 329 (1979).

⁵¹M. H. Chen, B. Crasemann, and H. Mark, Phys. Rev. A **24**, 147 (1981).